Biomacromol. J. Vol. 1, No. 2, 242-253, December 2015.

Biomacromolecular Journal
www.bmmj.org

Novel Pt(II) Complex and Its Pd(II) Aanalogue. Synthesis, Characterization, Cytotoxicity and DNA-interaction

S. Shahraki[a,*], H. Mansouri-Torshizi[b], M. Sadeghi[b], A. Divsalar[c] and A.A. Saboury[d]

[a]*Department of Chemistry, University of Zabol, Zabol, Iran*

[b]*Department of Chemistry, University of Sistan & Baluchestan, Zahedan, Iran*

[c]*Department of Biological Sciences,* Kharazmi *University, Tehran, Iran*

[d]*Institute of Biochemistry and Biophysics, University of Tehran, Tehran, Iran*

(Received 22 February 2016, Accepted 5 March 2016)

ABSTRACT

The ability of small molecules to perturb the natural structure and dynamics of nucleic acids is intriguing and has potential applications in cancer therapeutics. This work reports the synthesis, characterization, cytotoxicity and DNA-binding studies of two cytotoxic and intercalative $[M(bpy)(pyrr\text{-}dtc)]NO_3$ complexes (where M = Pt(II) and Pd(II), bpy = 2,2´-bipyridine and pyrr-dtc = pyrrolidinedithio-carbamate). Binding interaction of these complexes with calf thymus DNA (CT-DNA) was investigated by spectrophotometric, spectrofluorometric and gel filtration techniques. Gel filtration studies indicate that the binding of these complexes with CT-DNA is strong enough not to readily break. The binding constant and the thermodynamic parameters have been determined using absorption measurements. The fluorescence studies indicate that the two complexes bind to CT-DNA through an intercalative mode. The cytotoxic activity of these metal complexes has been tested against chronic myelocytic leukemia K562 cell lines and revealed much lower 50% cytotoxic concentration (C_{c50}) than that of cisplatin. We hope that such spectroscopic studies to be indeed helpful in studying the pharmacological response of drugs and design of dosage forms.

Keywords: Platinum(II)/palladium(II) complexes, DNA-binding, Intercalation, Cytotoxicity

INTRODUCTION

Cisplatin is an important cytotoxic drug used in the treatment of a variety of human cancers. Unfortunately, its clinical usefulness has frequently been limited by several negative side effects (nephrotoxicity, neurotoxicity, nausea, *etc*.) [1-3] and so it has stimulated and generated new areas of research, which mainly focused on the search for new metal-based complexes with lower toxicity and more improved therapeutic properties [4,5].

The strategy in pursuing the search for new drugs that combine high activity and low toxicity has been the coordination of planar ligands to platinum. This may result in an interesting biological activity because of the possible ability of the new metal complexes to inhibit DNA replication through single or simultaneous interactions such as intercalation and/or covalent coordination to DNA [6,7]. Complexes of the type $[Pt(N\text{-}N)(L\text{-}L)]^{n+}$ and $[Pt(N\text{-}N)L_2]^{n+}$ [8-10], where N-N is a rigid aromatic bidentate ligands, L-L is a non-aromatic bidentate ligand and L a monodentate ligand, can be potent intercalators to DNA. In this type of complexes the ancillary ligands L-L and L may play a major role on the interaction.

Dithiocarbamates have shown promising results in reversing the renal cellular damage caused by cisplatin in several animal models [11]. These ligands selectively remove the platinum metal from the enzyme-thiol complex without reducing the antitumor effect of the drug [12]. Trevisan and co-workers found Pd(II) dithiocarbamates to have anticancer activity like cisplatin with the additional advantage of no cross-resistance [13].

The present paper involves synthesis and characterization of two water soluble and structurally related platinum(II) and palladium(II) complexes (see Fig. 1). Both complexes bear a planar 2,2'-bipyridine ligand. This planar aromatic ligand along with square planar

*Corresponding author. E-mail: somaye_shahraki@yahoo.com

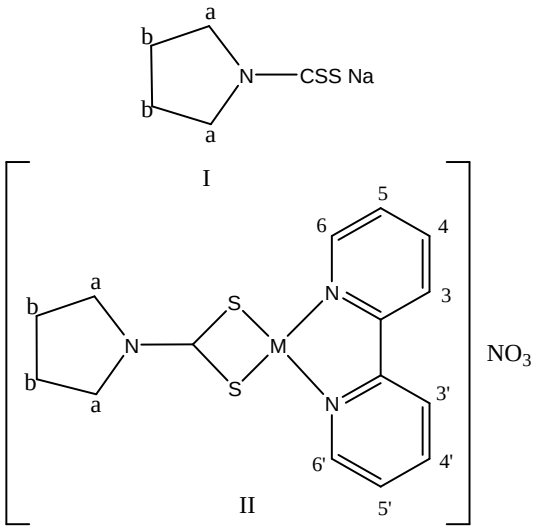

Fig. 1. Proposed structures and NMR numbering scheme of (I) pyrr-dtcNa, (II) $[M(bpy)(pyrr\text{-}dtc)]NO_3$.

geometry around Pt(II) or Pd(II) centers may make the complexes susceptible to intercalate in DNA. Moreover, we attached a bidentate dithocarbamate to Pt(II) and Pd(II) center which can protect a variety of animal species from renal, gastrointestinal and bone marrow toxicity induced by cisplatin [14]. These complexes have been tested against chronic myelogenous leukemia K562 cell line. In order to confirm the mode of binding of these complexes to CT-DNA, detailed interaction studies of them with CT-DNA are attempted.

EXPERIMENTAL

Chemicals and Apparatus

All reagents were commercially available (Aldrich or Merck) and used as supplied. Solvents were purified according to standard procedures [15].

The stock solution of DNA (4 mg ml^{-1}) was prepared by dissolving of DNA in Tris-HCl buffer with 20 mM NaCl at pH 7.0 overnight and was stored at 277 K for about a week. A solution of calf thymus DNA in the buffer gave a ratio of UV absorbance at 260 and 280 nm 0f ~1.8-1.9:1, indicating that the DNA was sufficiently free of protein. The concentration of DNA solution was determined from UV absorption at 260 nm using a molar absorption coefficient ε = 6600 M^{-1} cm^{-1}. The stock solutions of Pd(II)/Pt(II) complexes (0.5 mM) were made in Tris-HCl buffer by gentle stirring and heating at 308 K. Other chemicals used were of analytical reagent or of higher purity grade. $[Pt/Pd(bpy)Br_2]$ was made similar to that of $[Pt/Pd(bpy)Cl_2]$ [16]. Elemental analyses were performed using a Herause CHNO-RAPID elemental analyze. Electronic absorption spectra were recorded on a J_{ASCO} UV-Vis-7850 recording spectrophotometer. Infrared spectra (4000-400 cm^{-1}) were recorded using a J_{ASCO}-460 Plus FT-IR spectrometer in KBr disk. ^1H NMR spectra were recorded on a Brucker DRX-500 Avance spectrometer at 500 MHz in DMSO-d_6 using tetramethylsilane as internal reference. Fluorescence measurements were performed with a Varian spectro-fluorimeter model Cary Eclips. The melting points of the compounds were determined on a Unimelt capillary melting point apparatus. Conductivity measurements of the above platinum and palladium complexes were carried out on a Systronics Conductivity Bridge 305, using a conductivity cell of cell constant 1.0 and doubly distilled water was used as solvent.

Synthesis of Platinum(II) and Palladium(II) Complexes

Almost same procedure were used to prepare both complexes: $[M(bpy)Cl_2]$ (M = Pt(II) and Pd(II)) (0.5 mmol) was suspended in 100 ml acetone-water (2:1 v/v) mixture, and (1 mmol) of $AgNO_3$ was added to it with constant stirring. This reaction mixture was heated with stirring under dark for 6 h at 60 °C and then for 16 h at room temperature. The AgCl precipitate was filtered through Whatman 42 filter paper. To the clear yellow filtrate containing $[M(bpy)(H_2O)_2](NO_3)_2$, a solution of 0.5 mmol pyrrolidinedithiocarbamate sodium salt (this ligand was prepared by a literature method) [17] in 15 ml water was slowly added. Stirring was continued at ~50 °C for another 6 h and filtered. The clear yellowish orange filtrate was evaporated at 40-45 °C to complete dryness. The residue obtained was stirred with 15 ml acetone to get fine powder. The acetone was decanted and the process was repeated with the second portion of acetone to remove most of the impurities. A yellow precipitate was obtained and

recrystallized in dichloromethane/methanol (1:1) solvent mixture and then dried in vacuum under KOH pellets.

Characterization Data

2,2´-Bipyridinepyrrolidinedithiocarbamatoplatinum (II) nitrate: [Pt(bpy)(pyrr-dtc)]NO_3. Yield: 41% (0.114 g) of orange solid and decomposed at 293-296 °C. Anal. Calcd. for $C_{15}H_{16}N_4O_3S_2Pt$ (559): C, 32.20; H, 2.86; N, 10.02%. Found: C, 32.27; H, 2.85; N, 10.01%. IR (KBr), ν (cm^{-1}): 1546 (N-CSS), 1158 (CN-C), 943 $(CSS)_{as}$, 619 $(CSS)_s$ and 1380 (NO_3) [18-20]. Molar conductance measurement for the complex is 127 Ω^{-1} mol^{-1} cm^2 indicating 1:1 electrolytes [21]. ^{1}H NMR (DMSO-d_6, ppm, t = triplet, m = multiple, d = doublet) 3.72 (t, 4H, H_a), 2.05 (t, 4H, H_b), 8.70 (d, 2H, $H_{6,6'}$), 8.47 (m, 2H, $H_{4,4'}$), 8.42 (m, 2H, $H_{5,5'}$) and 7.70 (t, 2H, $H_{3,3'}$). Electronic spectra exhibit four bands. The bands at 220 nm (logε = 2.01), 283 nm (logε = 2.65), 321 nm (logε = 2.43) and 365 nm (logε = 3.02) may be assigned to intraligand π→π* and n→π* transitions of 2,2´-bipyridine ligand as well as CSS^- group [14].

2,2´-Bipyridinepyrrolidinedithiocarbamatopalladium (II) nitrate: [Pd(bpy)(pyrr-dtc)]NO_3. Yield: 65 % (0.153 g) of orange solid and decomposed at 272-276 °C. Anal. Calcd. for $C_{15}H_{16}N_4O_3S_2Pd$ (470): C, 38.30; H, 3.41; N, 11.90%. Found: C, 38.35; H, 3.45; N, 11.95%. IR (KBr), ν (cm^{-1}): 1532 (N-CSS), 1158 (CN-C), 943 $(CSS)_{as}$, 648$(CSS)_s$ and 1350(NO_3) [18-20]. Molar conductance measurement for the complex is 128.6 Ω^{-1} mol^{-1} cm^2 indicating 1:1 electrolytes [21]. ^{1}H NMR (DMSO-d_6, ppm, t = triplet, m = multiple, d = doublet) 3.55 (t, 4H, H_a), 2.05 (t, 4H, H_b), 8.66 (d, 2H, $H_{6,6'}$), 8.14 (m, 2H, $H_{4,4'}$), 7.69 (m, 2H, $H_{5,5'}$) and 8.37 (d, 2H, $H_{3,3'}$). Electronic spectra exhibit four bands. The bands at 248 nm (logε = 3.14), 305 nm (logε = 2.68) and 314 nm (logε = 2.70) and 373 nm (logε = 2.71) may be assigned to intraligand π→π* and n→π* transitions of 2,2´-bipyridine ligand as well as CSS^- group [14].

Biological Test

[Pt/Pd(bpy)(pyrr-dtc)]NO_3 complexes were screened for their anti-tumor activities against chronic myelogenous leukemia K562 cell line [22]. In this experiment, the clear stock solution (2 mM, in deionized water) was sterilized by filtering through sterilizing membrane (0.1 nm) and then varying concentrations of the sterilized drug (0-250 μM) were added to harvested cells.

UV-Vis Absorbance

The DNA-binding and denaturation experiments were performed separately at two temperatures 300 and 310 K in Tris-HCl buffer medium (20 mM, PH 7.0) containing 20 mM sodium chloride. The procedure followed to determine binding and thermodynamic parameters were similar to what was reported earlier [23,24].

Fluorescence Measurements

For fluorescence experiment, DNA was pretreated with ethidium bromide (EBr) and then platinum(II)/palladium(II) complexes were added to this mixture and their effect on the emission intensity was measured. In this experiment, maximum quantum yield for ethidium bromide was achieved at 471 nm, so we selected this wavelength as excitation radiation for all of the samples at different temperatures (300 and 310 K) and emission was observed in the range of 540-700 nm. The fluorescence Scatchard plot was performed to study the binding constant determination by the fluorescence titration method [25]. These experiments were carried out in Tris-HCl buffer of pH 7.0.

RESULTS AND DISCUSSION

Cytotoxicity Assay

In Fig. 2 the cell growth (in %) versus concentration (μM) of [Pt/Pd(bpy)(pyrr-dtc)]NO_3 complexes is represented. The 50% cytotoxic concentration (Cc_{50}) of each compound was determined 73 μM and 59 μM for Pt(II) and Pd(II) complexes, respectively. Moreover the Cc_{50} value of cisplatin under the same experimental conditions was determined to be 154 μM which is much higher than that of the two prepared complexes. However, the Cc_{50} values of these complexes are higher than that of our analogous palladium(II) dithiocarbamate complexes reported earlier [26].

Thermodynamics of CT-DNA-denaturation

The DNA concentration per nucleotide was determined by absorption spectroscopy using the known molar extinction coefficient value of 6600 M^{-1} cm^{-1} at 260 nm [27]. DNA-denaturation experiment was done by looking at

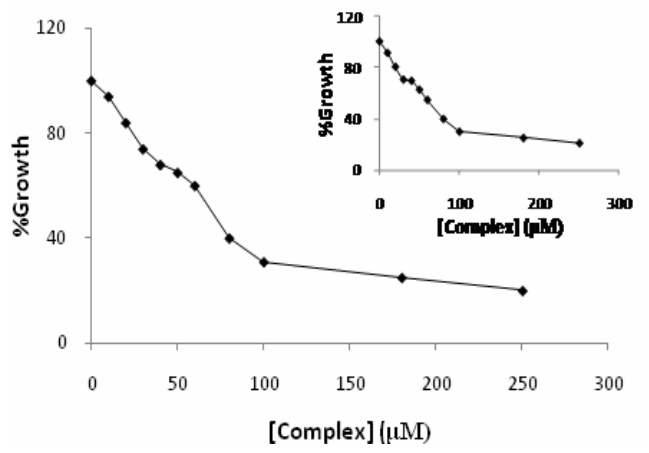

Fig. 2. The growth suppression activity of [Pt(bpy)(pyrr-dtc)]NO_3 and the insert, [Pd(bpy)(pyrr-dtc)]NO_3 on K562 cell line. The tumor cells were incubated with varying concentrations of the complexes for 24 h.

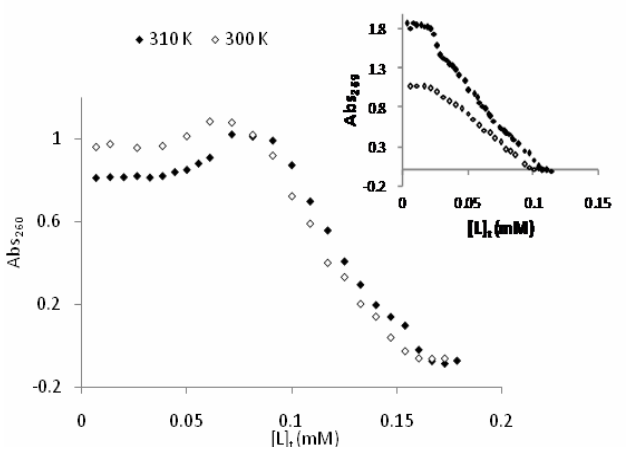

Fig. 3. The changes of absorbance of CT-DNA at λ_{max}= 260 nm due to increasing the total concentration of [Pt(bpy)(pyrr-dtc)]NO_3 and the insert, [Pd(bpy)(pyrr-dtc)]NO_3, $[L]_t$, at constant temperature of 300 and 310 K.

the changes in the UV absorption spectrum of DNA solution at 260 nm upon addition of platinum(II)/palladium(II) complexes. Addition of metal complex to DNA solution was continued until no further changes in the absorption readings were observed. These absorption readings of DNA solutions were plotted separately versus different concentrations of metal complexes at two temperatures of 300 and 310 K. The profiles of denaturation of CT-DNA by Pt(II)/Pd(II) complexes at 300 and 310 K and the values of $L_{1/2}$ so obtained are shown in Fig. 3 and Table 1. The significant observation of this experiment is the low values of $[L]_{1/2}$ for these complexes *i.e.* both complexes (in particular Pd(II) complex) can denature DNA at low concentrations. Thus, if these complexes will be used as anti-tumor agents, low doses will be needed, which may have fewer side effects [28-30].

Furthermore, some thermodynamic parameters found in the process of DNA denaturation are discussed here: Using the DNA denaturation plots and the Pace method [31], the values of K, unfolding equilibrium constant and ΔG°, unfolding free energy of DNA at two temperatures of 300 and 310 K in the presence of platinum(II) and palladium(II) complexes have been calculated by using Eqs. (1) and (2):

$$K = (A_N - A_{obs})/(A_{obs} - A_D) \quad (1)$$

$$\Delta G = -RT\ LnK \quad (2)$$

Where A_{obs} is absorbance readings in transition region, A_N and A_D are absorbance readings of nature and denatured conformation of DNA, respectively. A straight line is obtained when ΔGs are plotted *vs.* concentrations of metal complex in transition region at 300 and 310 K separately (These plots are shown in Fig. 4 for Pt(II) and the inset for Pd(II) systems). The equation for these lines can be written as follows [32,33]:

$$\Delta G = \Delta G(H_2O) - m[complex] \quad (3)$$

Where $\Delta G_{(H_2O)}$ is conformational stability of DNA in the absence of metal complex and m is a measure of the metal complex ability to denature DNA (see Table 1). The values of m for Pd(II) complex are higher than those of Pt(II) complex which indicate the higher ability of Pd(II) to denature DNA. These m values are similar to those of Pd(II) complex as well as surfactant reported earlier [34]. As we know, the higher the value of ΔG, the larger the conformational stability of DNA. However, the values of ΔG decrease by increasing the temperature for both complexes (see Table 1). This is based on expectations

Table 1. Thermodynamic Parameters and Values of $L_{1/2}$ of CT-DNA Denaturation by Palladium(II) and Platinum(II) Complexes

Compound	Temperature (K)	$L_{1/2}$	m (kJ mol^{-1})$(mM)^{-1}$	ΔG° (H_2O) (kJ mol^{-1} K^{-1})	ΔH° (H_2O) (kJ mol^{-1})	ΔS° (H_2O) (kJ mol^{-1})
	300	0.124	70.10	14.91		0.067
$[Pt(bpy)(pyrr\text{-}dtc)]NO_3$	310	0.119	107.7	14.23	35.15	0.067
	300	0.066	182.3	14.87		0. 067
$[Pd(bpy)(pyrr\text{-}dtc)]NO_3$	310	0.063	194.8	14.19	35.11	0.067

Table 2. Values of ΔA_{max} and Binding Parameters in the Hill Equation for Interaction between CT-DNA and Pd(II)/Pt(II) Complexes in 20 mM Tris-HCl Buffer and pH 7.0

Compound	T (K)	ΔA_{max}	G	K 10^3 $(M)^{-1}$	n	Error[a]
$[Pt(bpy)(pyrr\text{-}dtc)]NO_3$	300	0.106	4	23.21	2.28	0.0010
	310	0.134	4	25.80	3.06	0.0002
$[Pd(bpy)(pyrr\text{-}dtc)]NO_3$	300	0.083	5	77.15	2.98	0.0060
	310	0.253	5	94.82	3.94	0.0010

[a]Maximum error between theoretical and experimental values of ν.

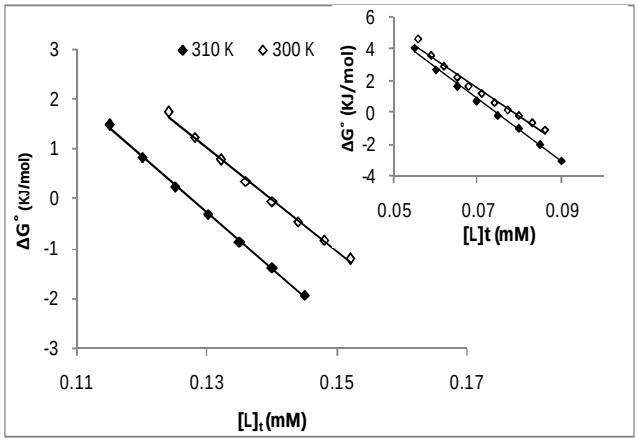

Fig. 4. The molar Gibbs free energies plots of unfolding (ΔG° *vs.* $[L]_t$) of CT-DNA in the presence of $[Pt(bpy)(pyrr\text{-}dtc)]NO_3$. Insert: in the presence of $[Pd(bpy)(pyrr\text{-}dtc)]NO_3$.

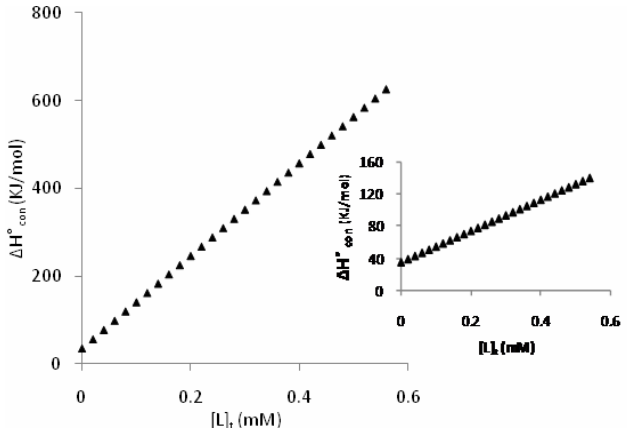

Fig. 5. Plots of the molar enthalpies of CT-DNA denaturation ($\Delta H^{\circ}_{conformation}$ or ΔH°_{con}) in the interaction with $[Pt(bpy)(pyrr\text{-}dtc)]NO_3$ and the insert with $[Pd(bpy)(pyrr\text{-}dtc)]NO_3$ complexes in the range of 300-310 K.

because in general, most of the macromolecules are less stable at higher temperature.

Molar enthalpy of CT-DNA denaturation in bsence of Pt(II) and Pd(II) complexes, $\Delta H_{(H_2O)}$, is another important thermodynamic parameter. To found this, we calculated the molar enthalpy of CT-DNA denaturation in presence of the metal complexes, $\Delta H_{conformation}$ or $\Delta H_{denaturation}$, in the range of two temperatures using Gibbs-Helmholtz equation as follows [35]:

$$\Delta H = \frac{\frac{\Delta G_{T_1}}{T_1} - \frac{\Delta G_{T_2}}{T_2}}{\frac{1}{T_1} - \frac{1}{T_2}} \quad (4)$$

On plotting the values of these enthalpies versus the concentration of metal complexes, straight lines will be obtained which are shown in Fig. 5 for [Pt(bpy)(pyrr-dtc)]NO_3 and the inset for [Pd(bpy)(pyrr-dtc)]NO_3 complexes. Intrapolation of these lines gives the values of $\Delta H_{(H_2O)}$ (Table 1). These plots show that in the range of 300-310 K the changes in the enthalpies in presence of Pt(II) and Pd(II) complexes are ascending. These observations indicate that, on increasing the concentration of Pt(II) and Pd(II) complexes, the stability of CT-DNA is increased. Moreover, the entropy $\Delta S_{(H_2O)}$ of DNA unfolding by Pt(II) and Pd(II) complexes have been calculated using equation $\Delta G = \Delta H - T\Delta S$, and the data are given in Table 1. These data show that the metal-DNA complex is more disordered than that of native DNA, because the entropy changes are positive for Pt(II)- or Pd(II)-DNA complexes in the denaturation processes of CT-DNA. These thermodynamic parameters compare favorably well with those of palladium(II) complexes as reported earlier [23,36].

Elucidation of CT-DNA Binding Parameters

Electronic absorption spectroscopy is one of the most useful techniques for examining the binding modes of metal complexes with DNA. The binding propensity of the complexes to CT-DNA was determined by monitoring the change of the absorption intensities of complexes Pt(II) and Pd(II) with the increasing concentration of CT-DNA in Tris-HCl buffer, pH 7.0 and total volume of 2 ml at 300 and 310 K. The values of ΔA, change in the absorbance when all binding sites on DNA were occupied by metal complex, are given in Table 2 and Fig. 6. These values were used to calculate the concentration of metal complex bound to DNA, $[L]_b$ and the concentration of free metal complex, $[L]_f$ and ν, the ratio of the concentration of bound metal complex to total [DNA] in the next experiment, that is, titration of fixed amount of DNA with varying amounts of each metal complex in total volume of 2 ml.

Using these data (ν and $[L]_f$), the Scatchard plots were constructed for the interaction of each metal complex at two temperatures of 300 and 310 K. The Scatchard plots are shown in Fig. 7 for [Pt(bpy)(pyrr-dtc)]NO_3 and the inset for [Pd(bpy)(pyrr-dtc)]NO_3. These plots are curvilinear concave downwards, suggesting cooperative binding [37]. On substituting ν and $[L]_f$ in Hill equation [$\nu = g(K[L]_f)^n/(1 + (K[L]_f)^n)$] we get a series of equation with unknown parameters n, K and g. Using Eureka software [38], the theoretical values of these parameters could be deduced (see Table 2). The K, apparent binding constant in the interaction of [Pd(bpy)(pyrr-dtc)]NO_3 with DNA is higher than that of [Pt(bpy)(pyrr-dtc)]NO_3 with DNA (see Table 2). This indicates that the interaction affinity of Pd(II) complex to DNA is more than Pt(II) complex. Because palladium complexes are about 10^5 times more labile than their platinum analogs [39]. Values of n, the Hill coefficient (as a criterion of cooperatively), for palladium complex are higher than that of platinum analog. Similar trends are observed in the results of cytotoxic studies of these two compounds.

Figure 7 also shows the experimental values of ν obtained from Scatchard (lines) and theoretical values of ν from Hill (dots) and their superimposability on each other. Moreover, these values of ν were plotted *vs.* the values of $Ln[L]_f$. The results are sigmoidal curves and are shown in Fig. 8 for Pt(II) complex and the inset for Pd(II) complex at 300 and 310 K. These plots indicate positive cooperative binding at both temperatures for both complexes. Finding the area under the above plots of binding isotherms and using Wyman-Jons equation [40], $\int \nu d\mathrm{Ln}[L]_f = \mathrm{Ln}[1 + K_{app}[L]_f^{\nu}$, (where $[L]_f$ and K_{app} are concentration of free metal complex and apparent binding constant for each particular ν, respectively) the values of K_{app} can be calculated at the two temperature 300 and 310 K for each particular ν [24]. Using the values of K_{app}, we can determine

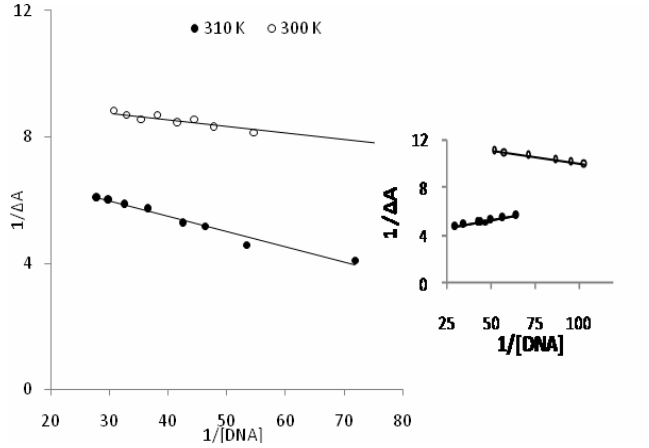

Fig. 6. The changes in the absorbance of fixed amount of metal complexes in the interaction with varying amount of CT-DNA at 300 and 310 K. The linear plot of the reciprocal of ΔA *vs.* the reciprocal of [DNA] for [Pt(bpy)(pyrr-dtc)]NO_3. Insert: for [Pd(bpy)(pyrr-dtc)]NO_3.

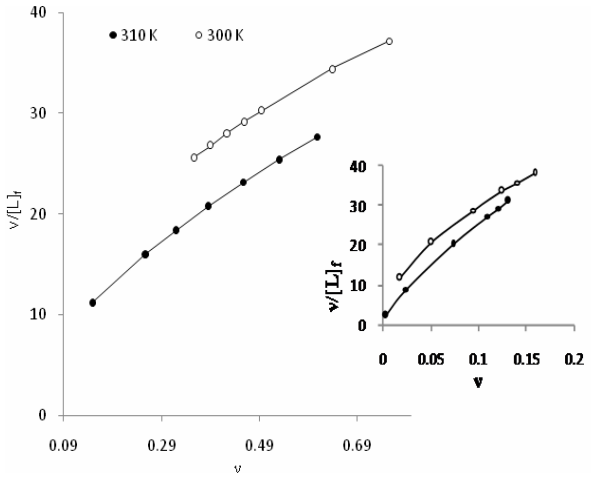

Fig. 7. Scatchard plots for binding of [Pt(bpy)(pyrr-dtc)]NO_3 with CT-DNA. The insert is Scatchard plots for binding of [Pd(bpy)(pyrr-dtc)]NO_3 with DNA.

the corresponding values of molar Gibbs free energy of binding ΔG_b molar enthalpy of binding ΔH_b and molar entropy of binding ΔS_b from (5), (6) and (7) Eqs.:

$$\Delta G_b = -RTLnK_{app} \quad (5)$$

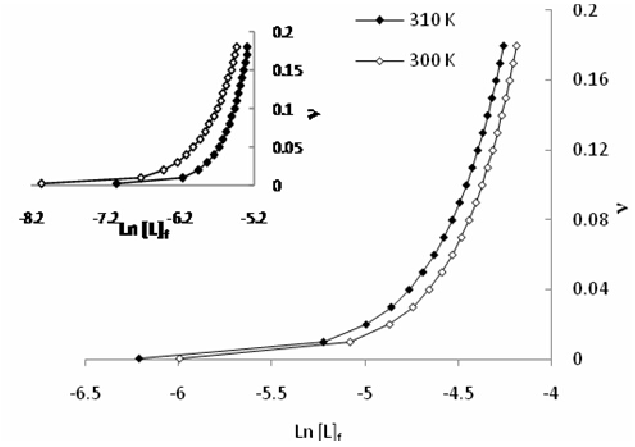

Fig. 8. Binding isotherm plots for [Pt(bpy)(pyrr-dtc)]NO_3 in the interaction with CT-DNA. Insert: for [Pd(bpy)(pyrr-dtc)]NO_3.

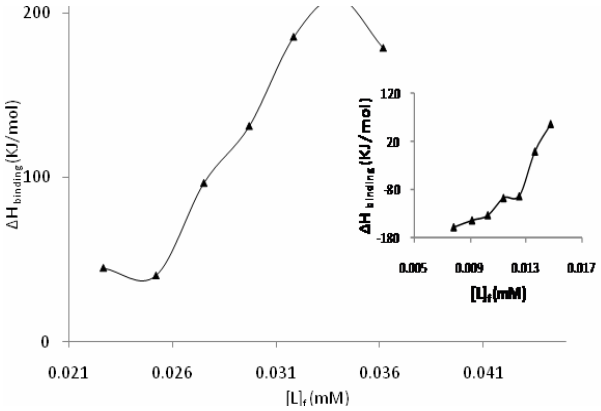

Fig. 9. Molar enthalpies of binding in the interaction between CT-DNA and [Pt(bpy)(pyrr-dtc)]NO_3 (Insert: [Pd(bpy)(pyrr-dtc)]NO_3 *vs.* free concentrations of complexes at pH 7.0 and 300 K.

$$Ln\frac{K_{app}T_1}{K_{app}T_1} = \frac{-\Delta H_b}{R(\frac{1}{T_2} - \frac{1}{T_1})} \quad (6)$$

$$\Delta G_b = \Delta H_b - T\Delta S_b \quad (7)$$

Plots of the values of ΔH_b *vs.* the values of $[L]_f$ are shown in Fig. 9 for [Pt(bpy)(pyrr-dtc)]NO_3 and the inset for

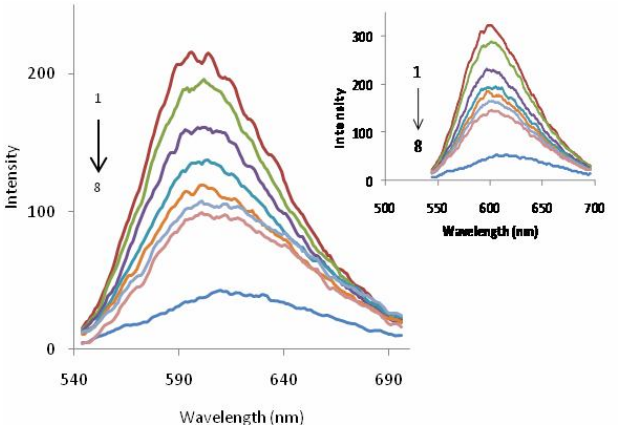

Fig. 10. Fluorescence emission spectra of interacted EBr-DNA in the absence (1) and presence of different concentrations of [Pt(bpy)(pyrr-dtc)]NO_3 and the inset for [Pd(bpy)(pyrr-dtc)]NO_3: 20 µM (2), 40 µM (3), 60 µM (4), 80 µM (5), 100 µM (6), 120 µM (7), EBr alone (8).

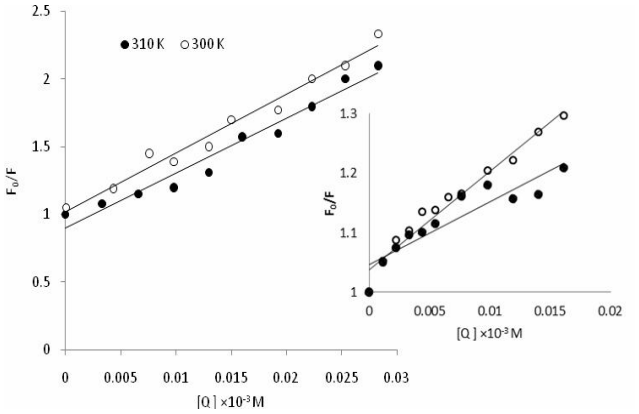

Fig. 11. Stern-Volmer plots for the interaction of [Pt(bpy)(pyrr-dtc)]NO_3 and CT-DNA (the inset for [Pd(bpy)(pyrr-dtc)]NO_3) at 300 and 310 K.

[Pd(bpy)(pyrr-dtc)]NO_3 at 300 K. Deflections are observed in both plots. These deflections indicate that at particular $[L]_f$, there is a sudden change in enthalpy of binding which may be due to binding of metal complex to macromolecule or macromolecule denaturation. Similar observations can be seen in the literature where Pd(II)/Pt(II) complexes have been interacted with CT-DNA [23,36].

Fluorescence Spectroscopic Studies

[Pt/Pd(bpy)(pyrr-dtc)]NO_3 complexes, however, are non-fluorescent on excitation in the visible region. Hence, competitive binding studies using ethidium bromide (EBr) bound to CT-DNA were carried out for Pt(II)/Pd(II) complexes. Ethidium bromide is a well-known cationic dye widely used as probe for native DNA [41]. The fluorescence intensity of EBr is very weak, but it is greatly increased when EBr is specially intercalated into the base pairs of double stranded DNA. It was previously reported that the fluorescent light could be quenched by the addition of a second molecule [42,43]. The quenching extent of fluorescence of EBr bound to DNA is used to determine the extent of binding between the second molecule and DNA. The emission spectra of EBr bound to DNA in the absence and the presence of [Pt(bpy)(pyrr-dtc)]NO_3 and [Pd(bpy)(pyrr-dtc)]NO_3 are given in Fig. 10. This figure show a significant reduction of the ethidium emission intensity by adding different concentrations of Pd(II) and Pt(II) complexes. It indicates that the fluorescence intensity of DNA intercalated ethidium bromide is quenched when ethidium is removed from the duplexes of DNA by the action of palladium or platinum complexes and is released into buffer medium. Thus it allows us to conclude that our two complexes possibly intercalate in DNA through the planar bpy ligand with coplanar positively charged square planar geometry around Pd(II) center.

It has been reported that there are two quenching types in characterizing the binding mechanism of quencher and macromolecules: static and dynamic (or collision) quenching. Static quenching refers to the formation of a non-fluorescence fluorophore-quencher complex, and the dynamic quenching refers to the quencher diffused to the fluorophore during the lifetime of the exited state upon contact, the fluorophore returns to ground state without emission of a photon. They can be distinguished by their different temperature dependence. To elucidate the quenching mechanism the Stern-Volmer equation is often applied:

$$\frac{F_0}{F} = 1 + K_q \tau_0 [Q] = 1 + K_{SV} \quad (8)$$

where F_0 and F are the fluorescence intensity in the absence

Table 3. Binding Parameters of CT-DNA Interaction with Pd(II)/Pt(II) Complexes

Compound	T (K)	K_{SV} (10^5 M^{-1})	K_q 10^{13} $(Ms)^{-1}$	K_b (10^4 M^{-1})	n
$[Pt(bpy)(pyrr\text{-}dtc)]NO_3$	300	3.17	3.17	5.67	3.32
	310	2.84	2.84	4.13	3.02
$[Pd(bpy)(pyrr\text{-}dtc)]NO_3$	300	4.54	4.54	6.88	2.56
	310	2.17	2.17	4.09	3.33

Table 4. Binding Parameters for Palladium(II) and Platinum(II) Complexes on the Fluorescence of EBr in the Presence of CT-DNA

Compound	r_f	K 10^5 $(M)^{-1}$	n
	0.00	0.242	
	0.25	0.167	
$[Pt(bpy)(pyrr\text{-}dtc)]NO_3$	0.50	0.088	0.0075
	0.75	0.062	
	0.00	0.270	
	0.16	0.170	
$[Pd(bpy)(pyrr\text{-}dtc)]NO_3$	0.33	0.109	0.0068
	0.50	0.08	

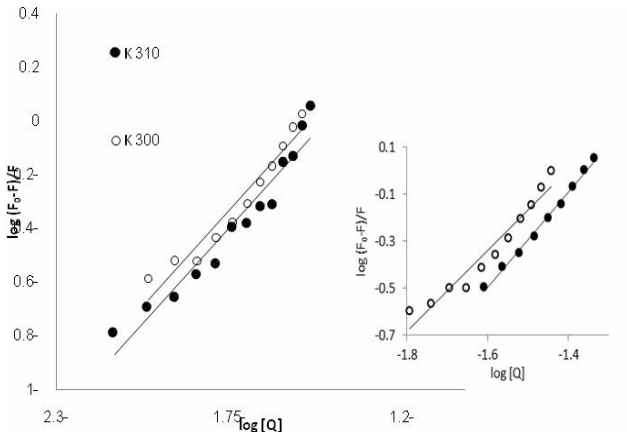

Fig. 12. Plots of $\log(F_0 - F)/F$ against log[complex] for $[Pt(bpy)(pyrr\text{-}dtc)]NO_3$ quenching effect on EBr-DNA fluorescence at 300 and 310 K (The inset for $[Pd(bpy)(pyrr\text{-}dtc)]NO_3$).

and presence of quencher (here Pd(II)/Pt(II)complex), respectively, K_q is the EBr-DNA quenching constant; τ_0 is the lifetime of the fluorophore in the absence of quencher and the fluorescence lifetime of the biopolymer is 10^{-8}, K_{sv} is the linear Stern-Volmer quenching constant, [Q] is the concentration of the quencher. The Stern-Volmer plots of DNA-Pd/Pt complex systems at 300 and 310 K are shown in Fig. 11 and the estimated parameters of Eq. (8) are listed in Table 3. Here, the values of K_q are much greater than the maximum diffusion collision quenching rate constant of various quenchers with the biomacromolecule. Thus, the quenching of EBr-DNA fluorescence occurred *via* a specific interaction between DNA and complexes, and static quenching is the dominant mechanism for both complexes [44]. Also, K_{sv} is inversely correlated with temperature, which indicates that the fluorescence quenching of DNA by

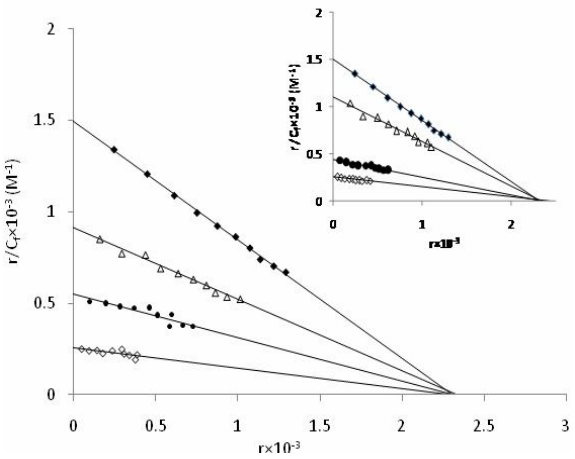

Fig. 13. Competition between [Pt(bpy)(pyrr-dtc)]NO_3 and the inset for [Pd(bpy)(pyrr-dtc)]NO_3 with ethidium bromide for the binding sites of CT-DNA (Scatchard plot). In curve no. 1 (♦), Scatchard plot was obtained with calf thymus DNA alone. Its concentration was 60 µM. In curves nos. 2 (Δ), 3 (●) and 4 (◊), respectively, 15, 30 and 45 µM for Pt(II) complex and 10, 20 and 30 µM, for Pd(II) complex were added, corresponding to molar ratio [complex]/[DNA] of 0.25, 0.5 and 0.75 for Pt(II) complex and 0.16, 0.33 and 0.5 for Pd(II) complex. Solutions were in 20 mM NaCl and 20 mM Tris-HCl (pH 7.0). Experiments were done at room temperature.

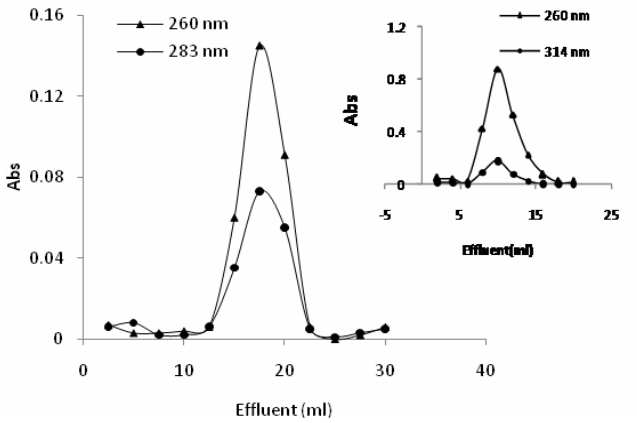

Fig. 14. Gel chromatograms of [Pt(bpy)(pyrr-dtc)]NO_3 and the inset for [Pd(bpy)(pyrr-dtc)]NO_3 obtained on Sephadex G-25 column, equilibrated with 20 mM Tris-HCl buffer of pH 7.0 in the presence of 20 mM sodium chloride.

above complexes**,** is not a dynamic process but a static process.

For static quenching, the relationship between fluorescence quenching intensity and the concentration of quenchers can be described by the binding constant formula:

$$\frac{\log((F_0 - F))}{F} = \log K_b + n \log[Q] \quad (9)$$

Where Q is the quencher, K_b and n are constant and number of binding sites; F_0 and F represent the fluorescence intensities in the absence and in the presence of quencher. A plot of $\log(F_0 - F)/F$ *vs.* $\log[Q]$ will give a straight line with a slope of n and y-axis intercept of $\log K_b$ (Fig. 12). The corresponding results at 300 and 310 K are shown in Table 3. The values of n approximate to 3, suggesting that three reactive sites exists in CT-DNA for both complexes**,** and are in good agreement with the results of above absorption experiments. The binding constants decreased with increasing temperature, which coincided with the Stern-Volmer quenching constants. Therefore, the probable quenching mechanism of Pd(II)/Pt(II) complexes with DNA-EBr binding reaction is initiated by compound formation rather than static quenching.

The fluorescence Scatchard plots obtained for competition of the Pt(II) and Pd(II) complexes with EBr to bind with DNA are given in Fig. 13. This figure shows that the above complexes inhibit competitively the EBr binding to CT-DNA (type-A behavior) [45], where number of binding sites n (intercept on the abscissa) remain constant and the slope of the graphs, that is K_{app} (apparent association constant) decreases with increasing the concentration of Pt(II) and Pd(II) complexes (Table 3). This implies that both complexes are intercalating in CT-DNA and thereby competing for intercalation sites occupied by EBr. The values of K_{app} and n, are listed in Table 4. Compare their K_{app} values with those of other known CT-DNA-intercalative complexes which possess analogical structure; Pt(II) and Pd(II) complexes in our paper have similar or stronger affinities with CT-DNA [36].

Gel Filtration Studies

[Pt/Pd(bpy)(pyrr-dtc)]NO_3 complexes were separately

incubated with CT-DNA for 2 h in Tris-HCl buffer, pH 7.0. DNA-metal complexes were then passed through a Sephadex G-25 column equilibrated with the same buffer. The elusion of the column fraction of 2.0 ml was monitored at 283 nm and 314 nm for Pt(II) and Pd(II) complexes and at 260 nm for interacted DNA-metal complexes [26,46]. These results are given in Fig. 14. This plot shows that the peak obtained for the two wavelengths are not resolved and suggests that CT-DNA has not separated from the metal complexes. Thus, it implies that the binding between CT-DNA and the metal complexes is not reversible under such circumstances. This is due to the fact that if the interaction between CT-DNA and metal complexes was weak, the CT-DNA should have come out of the column separately [47]. Also peaks due to DNA and each of the metal complexes should have appeared in different places of the plots. Thus the interaction affinities are not only effective but also strong enough not to break readily.

CONCLUSIONS

Two new [Pt(bpy)(pyrr-dtc)]NO_3 and [Pd(bpy)(pyrr-dtc)]NO_3 complexes have been successfully synthesized and characterized. Electronic absorption spectra, fluorescence spectra and gel filtration measurements studies indicate that these two complexes can strongly bind with CT-DNA, presumably *via* an intercalation mechanism. DNA-binding affinities of [Pd(bpy)(pyrr-dtc)]NO_3 are higher than [Pt(bpy)(pyrr-dtc)]NO_3. They exhibited potent cytotoxic properties against chronic myelogenous leukemia K562 cell line. The cells showed different sensitivities to complexes. Cc_{50} values of Pd(II) complex are lower than those of Pt(II) complex and both are lower than those of cisplatin. They unexpectedly denature CT-DNA at low concentrations. Determination of several binding and thermodynamic parameters has also been attempted.

REFERENCE

[1] A. Pasini, F. Zunino, Angew. Chem. Int. Ed. Engl. 26 (1987) 615.

[2] N. Farrell, Y. Que, M.P. Hacker, J. Med. Chem. 33 (1990) 2179.

[3] A.G. Sykes, Plat. Met. Rev. 32 (1988) 170.

[4] S.E. Sherman, S. Lippard, J. Chem. Rev. 87 (1987) 1153.

[5] E.J. Gao, L. Wang, M.C. Zhu, L. Liu, W.Z. Zhang, Eur. J. Med. Chem. 45 (2010) 311.

[6] K.E. Erkkila, D.T. Odom, K.J. Barton, J. Chem. Rev. 99 (1999) 2777.

[7] N. Farrell, Transition Metal Complexes as Drugs and Chemotherapeutic in: B.R. James, R. Ugo (Eds.), Catalysis by Metal Complexes, Kluwer, Dordrecht, 1989.

[8] M. Cusumano, A. Giannetto, J. Inorg. Biochem. 65 (1997) 137.

[9] C.M. Che, M. Yang, K.H. Wong, H.L. Chan, W. Lam, Chem. Eur. J. 5 (1999) 3350.

[10] M. Cusumano, M.L. Di Pietro, A. Giannetto, F. Nicolo, E. Rotondo, Inorg. Chem. 37 (1998) 563.

[11] S. Hidaka, M. Tsuruoka, T. Funakoshi, H. Shimada, M. Kiyozumi, S. Kojima, Ren. Fail. 16 (1994) 337.

[12] D.L. Bodenner, P.C. Dedon, P.C. Keng, R. Borch, Cancer Res. 46 (1986) 2745.

[13] A. Trevisan, C. Marzano, P. Cristofori, M.B. Venturini, L. Giovagnini, D. Fregona, Arch. Toxicol. 76 (2002) 262.

[14] R. Mital, N. Jain, T.S. Srivastava, J. Inorg. Chim. Acta 166 (1989) 135.

[15] A.I. Vogel, In A Textbook of Practical Organic Chemistry; 3rd ed.; Longman Scientific & Technical, 1989.

[16] F.A. Palocsay, J.V. Rund, Inorg. Chem. 8 (1969) 524.

[17] D.C. Menezes, F.T. Vieira, G.M. de-Lima, A.O. Porto, M.E. Cortés, J.D. Ardisson, T.E. Albrecht-Schmitt, Eur. J. Med. Chem. 45 (2005) 1277.

[18] L. Ronconi, L. Giovagnini, C. Marzano, *et al.*, Inorg. Chem. 44 (2005) 1867.

[19] A. Manohar, K. Ramalingam, G. Bocelli, L. Righi, Inorg. Chim. Acta 314 (2001) 177.

[20] L. Kumar, N.R. Kandasamy, T.S. Srivastava, A.J. Amonkar, M.K. Adwankar, M.P. Chitnis, J. Inorg. Biochem. 23 (1984) 1.

[21] W.J. Gearg, Coord. Chem. Rev. 7 (1971) 81.

[22] A. Divsalar, A.A. Saboury, R. Yousefi, A.A. Moosavi-Movahedi, H. Mansoori-Movahedi, H. Mansouri-Torshizi, Int. J. Biol. Macromol. 40 (2007)

381.

[23] M. Saeidfar, H. Mansouri-Torshizi, G.R. Behbehani, A.A. Saboury, A. Divsalar, B. Kor. Chem. Soc. 30 (2009) 1951.

[24] M. Islami-Moghaddam, H. Mansouri-Torshizi, A. Divsalar, A.A. Saboury, J. Iran. Chem. Soc. 6 (2009) 552.

[25] S. Satyanarayana, J.C. Dabrowiak, J.B. Chaires, Biochemistry 31 (1992) 9319.

[26] H. Mansouri-Torshizi, M. Islami-Moghaddam, A. Divsalar, A.A. Saboury, Acta Chim. Slov. 58 (2011) 811.

[27] M.F. Reichmann, S.A. Rice, C.A. Thomas, P. Doty, J. Am. Chem. Soc. 76 (1954) 3047.

[28] Z.H. Xu, F.J. Chen, P.X. Xi, X.H. Liu, Z.Z. Zeng, J. Photochem. Photobiol. A Chem. 196 (2008) 77.

[29] S.Z. Bathaie, A. Bolhasani, R. Hoshyar, B. Ranjbar, F. Sabouni, A.A. Moosavi-Movahedi, DNA Cell Biol. 26 (2007) 533

[30] L. Peres-Flores, A.J. Ruiz-Chica, J.G. Delcros, F.M. Sanches, F. Ramirez, J. Spectrochim. Acta A 69 (2008) 1089.

[31] R.F. Greene, C.N. Pace, J. Biol. Chem. 249 (1974) 5388.

[32] A.M.Q. King, B.H. Nicholson, Biochem. J. 114 (1969) 679.

[33] M. Ghadermarzi, A.A. Saboury, A.A. Moosavi-Movahedi, Polish J. Chem. 72 (1998) 2024.

[34] A.A. Saboury, A.K. Bordbar, A.A. Moosavi-Movahedi, B. Chem. Soc. JPN. 69 (1996) 3031.

[35] G.M. Barrow, Physical Chemistry of the Life Sciences, in Physical Chemistry, Graw-Hill, New York, 1988.

[36] H. Mansouri-Torshizi, M. Saeidifar, A. Divsalar, A.A. Saboury, J. Biomol. Struct. Dyn. 28 (2011) 805.

[37] A.A. Saboury, J. Iran. Chem. Soc. 3 (2006) 1.

[38] M.L. James, G.M. Smith, J.C. Wolford, Applied Numerical Methods for Digital Computer, New York, Harper and Row Publisher, 1985.

[39] M.P. Hacker, E.B. Douple, I.H. Krakoff, in: M.A. Nijhoff (Ed.), Platinum Coordination Complexes in Cancer Chemotherapy, Boston, 1984.

[40] H. Mansouri-Torshizi, M. Islami-Moghaddam, A.A. Saboury, Acta Biochim. Biophys. Sin. 35 (2003) 886.

[41] V.A. Izumrudov, M.V. Zhiryakova, A.A. Goulko, Langmuir 18 (2002) 10348.

[42] B.C. Baguley, M. LeBret, Biochemistry 23 (1984) 937.

[43] J.R. Lakowicz, G. Webber, Biochemistry 12 (1973) 4161.

[44] M. Howe-Grant, K.C. Wu, W.R. Bauer, S.J. Lippard, Biochemistry 15 (1976) 4339.

[45] H. Mansouri-Torshizi, T.S. Srivastava, H.K. Parekh, M.P. Chitnis, J. Inorg. Biochem. 45 (1992) 135.

[46] H. Mansouri-Torshizi, R. Mital, T.S. Srivastava, H. Parekh, M. P. Chitnis, J. Inorg. Biochem. 44 (1991) 239.